2008 American Control Conference
Westin Seattle Hotel, Seattle, Washington, USA
June 11-13, 2008

Remarks on Tracking and Robustness Analysis for MEM Relays

Michael Malisoff, Frédéric Mazenc, and Marcio de Queiroz

Abstract— **We announce a new class of tracking controllers, applicable to both electrostatic and electromagnetic microelectromechanical (MEM) relays, that yield arbitrarily fast local exponential convergence of the tracking error to zero and uniform global asymptotic stability of the error dynamics. Our stability analysis is based on an explicit, strict, global Lyapunov function construction. Our Lyapunov approach also leads to an input-to-state stability based quantification of the effects of parametric uncertainty on the tracking performance. The MEM dynamics contain a quadratic nonlinearity that leads to constraints on the class of reference trajectories that can be tracked. We illustrate how to craft a reference trajectory that is compatible with these constraints and with a typical opening and closing relay operation. Our simulation indicates the good tracking performance of our controllers.**

Key Words—**MEM relays, nonlinear control, Lyapunov theory, input-to-state stability**

I. Introduction

Several types of relays are used in industrial applications to close or open connections in electric circuits. Many industrial control processes use traditional mechanical relays, which are large, slow, and noisy. By contrast, solid-state relays have faster response, much longer lifetimes, and smaller sizes. However, solid-state relays have high power consumption and poor electrical isolation, because of their low off-resistance and high on-resistance. Reducing their on-resistance can increase output capacitance, which can cause other problems when there is switching of high-frequency signals [16].

Recent advances in the area of microelectromechanical systems (MEMS) have led to new opportunities for developing power and signal relays [16]. MEM relays have the same advantages as mechanical relays, viz., higher dielectric strength, lower power consumption, higher off-resistance, lower cost, and lower on-resistance. MEMS technology can also miniaturize mechanical relays, thereby treating the problems of switching time and size. Moreover, micro-relays can be used readily in conjunction with other electronic components.

There are two major classes of MEM relays, involving different methods of actuation: electrostatic and electromagnetic [2], [3], [4], [5], [12], [16]. Relays involve a control circuit and an output circuit. In electrostatic relays, the circuits use a common pair of parallel electrodes (one movable and the other fixed) which act as a capacitor; see Figure 1. Voltage applied across the electrodes yields an electric field between them, and then creates an attractive force between them. As the electrodes come together, so do the two contacts of the output circuit; this allows the flow of current and the closing of the circuit. In electromagnetic relays, the control circuit has an electromagnet whose magnetic force acts on a movable electrode located above the fixed coil post; see Figure 2. The magnetic force then attracts the electrode, and it closes the output circuit like in an electrostatic relay.

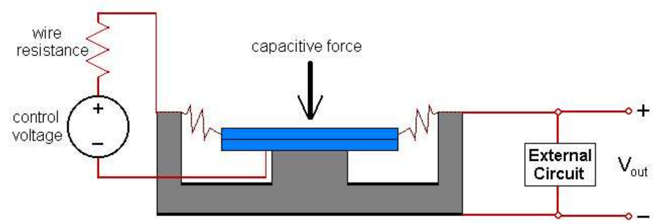

Fig. 1. Electrostatic MEMS Relay

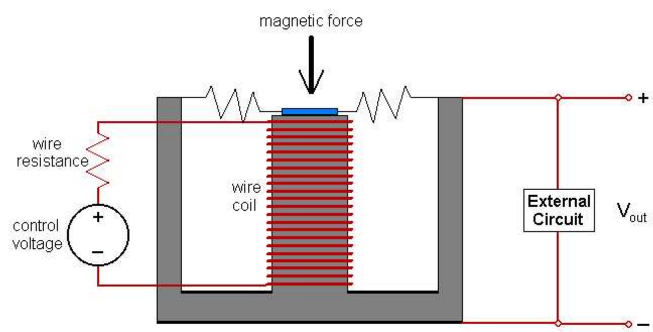

Fig. 2. Electromagnetic MEMS Relay

The electrostatic actuation method is more common for micro-relays [16]. This is largely due to difficulties in producing micro-size electromagnetic actuators. Another disadvantage in using electromagnetic actuation is that it requires more current, leading to larger heat generation and more power consumption. Nevertheless, [2] studies both actuation methods in their ability to produce micron and submicron precision under rapid motion, and it provides a strong rationale in favor of using magnetically-driven micro-actuators. See [5], [16] for a detailed review on the design and production of electromagnetic and electrostatic micro-relays.

Voltage-controlled MEM actuators produce an important

Supported by NSF/DMS Grants 0424011 and 0708084 (MM) and NSF/CAREER Grant 0447576 (MdQ).

M. Malisoff is with the Department of Mathematics, Louisiana State University, Baton Rouge, LA 70803-4918. malisoff@lsu.edu

F. Mazenc is with Projet MERE INRIA-INRA, UMR Analyse des Systèmes et Biométrie, INRA 2, pl. Viala, 34060 Montpellier, France. Frederic.Mazenc@supagro.inra.fr

Marcio de Queiroz is with the Department of Mechanical Engineering, Louisiana State University, Baton Rouge, LA 70803-6413. dequeiroz@me.lsu.edu

978-1-4244-2079-7/08/$25.00 ©2008 AACC.

nonlinear phenomenon associated with a saddle-node bifurcation [7], called *pull-in* [13]. A physical explanation of pull-in is as follows. Assume that the voltage across the MEM actuator is incrementally raised from zero. First the (capacitive or magnetic) force will pull the movable electrode down with increasing voltage. The voltage achieves a critical value, corresponding to an electrode displacement of $1/3$ the nominal (zero-voltage) gap. The movable electrode then suddenly 'crashes' onto the bottom electrode. This problem is especially detrimental in MEM relays, because they necessarily operate in the pull-in region when the relay closes [17]. Clearly, repeated occurrence of pull-in will damage the micro-relay. The pull-in phenomenon implies that MEM *relays* (as opposed to MEM actuators in general) should not be operated in open loop. Rather, a *feedback* controller is needed for the relay to properly close and open without damaging the device.

Most MEM actuator feedback control studies have largely been devoted to the electrostatic case. In [7], [8], [9], partial-state feedback controls were proposed using charge and position with a velocity observer. Control schemes based on backstepping, control Lyapunov functions, differential flatness, and input-to-state stabilization were provided in [18], [19]. A PD-type controller was reported in [1] for a MEM electrostatically-actuated optical switch. In [17], a common nonlinear dynamic structure was developed for voltage-controlled electromagnetic and electrostatic MEM relays. Also, [17] provided two nonlinear state feedback control schemes: a feedback linearization tracking controller and a Lyapunov-based setpoint controller.

In this note, we announce a new class of controllers for electrostatic and electromagnetic voltage-driven MEM relays, based on the explicit construction of Lyapunov functions and state feedback. Then we use input-to-state stability (ISS) theory [14], [15] to quantify the robustness of our feedback controller to parametric uncertainty. This makes it possible to analyze the effects of parameter uncertainty on the tracking error. We validate our results in Section VI below in a simulation. For complete proofs of our results and extensions involving partial state feedback, see [10].

II. System Model

As noted in [17], electrostatic and electromagnetic micro-relays share the nonlinear dynamic model

$$\begin{aligned} m\ddot{x} + b\dot{x} + kx &= \alpha z^2 \\ \beta\dot{z} + \gamma(g_0 - x)z &= u, \end{aligned} \tag{1}$$

in which

$$z = \begin{cases} q \\ \phi \end{cases}, \quad \alpha = \begin{cases} 1/(2\epsilon A) \\ 1/(2\mu A) \end{cases}, \quad \beta = \begin{cases} R \\ N \end{cases}, \quad \text{and} \quad \gamma = \begin{cases} 1/(\epsilon A) \\ R/(N\mu A), \end{cases} \tag{2}$$

the upper (resp., lower) rows in (2) are for the electrostatic (resp., electromagnetic) micro-relay, x denotes the position of the movable electrode with $x = 0$ when it is in the open position, $m > 0$ denotes the movable electrode mass, $b > 0$ denotes the squeezed-film damping coefficient, $k > 0$ denotes the spring stiffness, $g_0 > 0$ is the gap when the movable electrode is in the open position, A denotes the movable electrode area, $R > 0$ denotes the resistance of the circuit, and $u = v$ where v is the input voltage. For the electrostatic micro-relay case, q is the charge, and ϵ is the gap permittivity. For the electromagnetic micro-relay case, ϕ is the flux, μ denotes the gap permeability, and N denotes the number of coil turns.

Remark 1: We assume in (1) that there is no contact between the electrodes in the micro-relay dynamics, meaning $x \in (-\infty, g_0)$. When contact occurs, the kinetic energy for the movable electrode is assumed to be zero so the dynamics becomes $\beta\dot{z} = u$ and $x \equiv g_0$; i.e., we do not allow bouncing by the movable electrode on the fixed electrode. See [11] for a dynamic model that allows contact bounce.

III. Tracking Control Design

In the sequel, all (in)equalities are to be understood to be true globally unless otherwise indicated. We omit the arguments of our functions when they are clear. By C^r, we mean r times continuously differentiable, and $|\cdot|$ is the Euclidean norm. By *properness* of W, we mean that $W(p) \to +\infty$ as $|p| \to +\infty$. Fix a C^3 function $y_d : [0,\infty) \to \mathbb{R}$ (called a *reference trajectory*) that admits constants $m_1, m_2, m_3, m_4 > 0$ that satisfy

$$\begin{aligned} &\text{(a)}\ \ m_1 \le y_d(t) \le m_2, \ \ |\dot{y}_d(t)| \le m_3, \\ &\quad\ \ \text{and}\ \ |\ddot{y}_d(t)| \le m_4 \ \ \forall t \ge 0, \ \text{and} \\ &\text{(b)}\ \ m_4 + \kappa_2 m_3 < 0.9\kappa_1 m_1 \end{aligned} \tag{3}$$

where $\kappa_1 = \frac{k}{m}$ and $\kappa_2 = \frac{b}{m}$ and the parameters come from (1). Our first objective is to design a controller $u(x, \dot{x}, z, t)$ that forces $x(t)$ to track $y_d(t)$ for all initial states $x(t_0) \in (-\infty, g_o)$. See Section V below for cases where there is uncertainty in the values of the model parameters; and see [10] for a Lyapunov-based stability analysis leading to our partial-state (i.e., no velocity measurement) stabilizing feedbacks for cases where only x and z can be measured. We require that u is C^1 in $(x, \dot{x}, z)$ and continuous in t. We wish to choose the feedback u so that it stabilizes x to y_d, and so that the stability has arbitrarily fast local exponential convergence.

Remark 2: The micro-relay stability problem is usually analyzed as a regulation/setpoint problem; i.e., using a piecewise constant command function that alternates the closing and opening of the relay. Here we construct *tracking* controllers because it provides the flexibility for selecting a reference trajectory that can improve the micro-relay performance. For example, one may wish to choose a *smooth* trajectory minimizing both the velocity of the movable electrode when it approaches the fixed electrode during closing and also overshoots during opening.

Remark 3: The structure of (1) leads to our conditions (3) on the reference trajectory, as we will show below. In

Section VI, we build a reference trajectory that is physically compatible with typical MEM relay operations while also satisfying (3).

To specify our control objective, consider the dynamics for $Y = (e_1, e_2, \zeta)$ in which $e_1 = x - y_d$, $e_2 = \dot{e}_1$,

$$\begin{aligned} &\zeta(t) = \sqrt{\tfrac{\alpha}{m}} z(t) - R_\mu(e_1(t), e_2(t), t), \\ &R_\mu(e_1, e_2, t) = \\ &\sqrt{\ddot{y}_d(t) + \kappa_2 \dot{y}_d(t) + \kappa_1 y_d(t) + \mu(e_1, e_2)}, \end{aligned} \tag{4}$$

and $\mu \in C^1$ will be specified to satisfy

$$|\mu(e_1, e_2)| \leq 0.1 \kappa_1 m_1 \tag{5}$$

everywhere. By (3) and (5),

$$\begin{aligned} 0 &< \underline{R} := \sqrt{0.9\kappa_1 m_1 - m_4 - \kappa_2 m_3} \\ &\leq R_\mu(e_1, e_2, t) \leq \sqrt{2\kappa_1 m_2} =: \overline{R}. \end{aligned} \tag{6}$$

When $\mu \equiv 0$, we write $R_0(t)$ to mean $R_\mu(e_1, e_2, t)$ because in that case there is no dependence on $e = (e_1, e_2)$. The new feedback

$$u = \gamma\,(g_0 - x)\, z + \beta v_1 \sqrt{m/\alpha} \tag{7}$$

and simple calculations give the $Y = (e_1, e_2, \zeta)$ dynamics

$$\left\{ \begin{array}{rcl} \dot{e}_1 &=& e_2 \\ \dot{e}_2 &=& -\kappa_1 e_1 - \kappa_2 e_2 + \mu(e_1, e_2) \\ && +\zeta^2 + 2\zeta R_\mu(e_1, e_2, t) \\ \dot{\zeta} &=& v_1 - \frac{1}{2R_\mu(e_1, e_2, t)} \{ \dddot{y}_d(t) + \kappa_2 \ddot{y}_d(t) \\ && +\kappa_1 \dot{y}_d(t) + \dot{\mu} \} \end{array} \right. \tag{8}$$

where $\dot{\mu}$ denotes the time derivative of μ along solutions of (8), namely,

$$\begin{aligned} \dot{\mu} \;=\; & \tfrac{\partial \mu}{\partial e_1}(e_1, e_2) e_2 + \tfrac{\partial \mu}{\partial e_2}(e_1, e_2) \left[-\kappa_1 e_1 - \kappa_2 e_2 \right. \\ & \left. + \mu(e_1, e_2) + \zeta^2 + 2\zeta R_\mu(e_1, e_2, t) \right]. \end{aligned} \tag{9}$$

We would like that for each constant $\mathcal{L} > 0$, there exists a $\mu \in C^1$ satisfying (5) and a continuous controller $v_1 = v_1(e_1, e_2, \zeta, t)$ (with μ and v_1 depending in general on $\mathcal{L}$) that is C^1 in (e_1, e_2, ζ) for which the following hold, in which $\underline{K}\mathcal{B}_3 = \{q \in \mathbb{R}^3 : |q| \leq \underline{K}\}$:

- S1 The closed loop system (8) with v_1 is uniformly globally asymptotically stable (UGAS) to 0 [6].
- S2 There are constants $\underline{K}, \overline{K} > 0$ such that for each $t_o \geq 0$ and all solutions $Y(t)$ of (8) (in closed loop with v_1) with initial states $Y(t_o) \in \underline{K}\mathcal{B}_3$,

$$|Y(t)| \leq \overline{K} e^{-\mathcal{L}(t - t_o)} |Y(t_o)| \quad \forall t \geq t_o \geq 0. \tag{10}$$

When these two objectives can be realized for each constant $\mathcal{L} > 0$, we say that the feedback (7) stabilizes x to y_d with *arbitrarily fast local exponential convergence*. Given any constant $a_2 > 0$ with $\overline{R}$ as defined in (6), set

$$\begin{aligned} &\Gamma = 16 \left[\sqrt{\tfrac{2}{\kappa_1}} + K \right]^2 \left(1 + \overline{R}^2 \right) + 1, \quad \text{where} \\ &K = \max \left\{ 2, \tfrac{2}{\kappa_1}, \tfrac{2}{\kappa_2} + \tfrac{(\kappa_2 + a_2)^2}{\kappa_1 \kappa_2} \right\}, \quad \text{and} \\ &\Theta = \tfrac{4}{\underline{R}} \left\{ 1 + \Gamma \left(\tfrac{1}{\kappa_1} + 1 \right) \right\}. \end{aligned} \tag{11}$$

The following theorem from [10] shows how our goals can be realized:

Theorem 1: Let a_1 and a_2 be any given positive constants and set $\sigma(s) = s/\sqrt{1 + s^2}$ and

$$\begin{aligned} &\mu(e_1, e_2) = \\ &-\tfrac{\kappa_1 m_1}{20} \left[\sigma\left(\tfrac{20 a_1}{\kappa_1 m_1} e_1 \right) + \sigma\left(\tfrac{20 a_2}{\kappa_1 m_1} e_2 \right) \right]. \end{aligned} \tag{12}$$

Then for any constant a_3 for which

$$a_3 \;\geq\; \Theta\{a_1 + a_2(1 + 2\overline{R} + \kappa_1 + \kappa_2 + a_1 + a_2)\}, \tag{13}$$

the feedback

$$\begin{aligned} v_1(e_1, e_2, \zeta, t) \;&=\; -a_3 \zeta (1 + \zeta^2) \\ +\tfrac{1}{2R_\mu(e_1, e_2, t)} &\{ \dddot{y}_d(t) + \kappa_2 \ddot{y}_d(t) + \kappa_1 \dot{y}_d(t) \} \end{aligned} \tag{14}$$

renders (8) UGAS to the origin. Moreover, for each constant $\mathcal{L} > 0$, we can choose values of the a_is and $\underline{K}, \overline{K} > 0$ so that all trajectories of (8) in closed loop with (14) that start in $\underline{K}\mathcal{B}_3$ satisfy (10). Hence, (7) with the choice (14) stabilizes x to y_d with arbitrarily fast local exponential convergence.

Remark 4: Our proof of Theorem 1 constructs an explicit strict Lyapunov function for (8) in closed loop with (14), namely,

$$\begin{aligned} &V_3(e_1, e_2, \zeta) = V_2(e_1, e_2) + \Gamma Q(\zeta), \quad \text{where} \\ &V_2(e_1, e_2) = e_1 e_2 + K V_1(e_1, e_2), \\ &Q(\zeta) = \tfrac{1}{a_3} \left(\tfrac{1}{2}\zeta^2 + \tfrac{1}{4}\zeta^4 \right), \\ &\quad V_1(e_1, e_2) = \tfrac{1}{2} e_2^2 \\ &\quad + \int_0^{e_1} \left\{ \kappa_1 l + \frac{\kappa_1 m_1}{20} \sigma\left(\frac{20 a_1}{\kappa_1 m_1} l \right) \right\} dl, \end{aligned} \tag{15}$$

Γ and K are from (11), and the positive constants a_i will be chosen later. Strict Lyapunov functions are very useful in a variety of applications, e.g., for quantifying the effects of parametric uncertainty. For example, our Lyapunov analysis shows that the tracking is robust to suitably small uncertainties in our parameters k and b, using the input-to-state stability paradigm; see Section V below.

Remark 5: Theorem 1 also holds (with the identical proof) with $\sigma(s) = s/\sqrt{1 + s^2}$ replaced by any C^2 function $\sigma : \mathbb{R} \to [-1, +1]$ satisfying (I) $\sigma(0) = 0$, $\sigma'(0) = 1$, and $0 \leq \sigma' \leq 1$ everywhere and (II) $s \mapsto s\sigma(s)$ is positive definite. We made our choice $\sigma(s) = s/\sqrt{1 + s^2}$ (which satisfies (I)-(II)) to make the statement of the theorem simpler. For a variant of Theorem 1 leading to partial-state (i.e., no velocity measurement) stabilizing feedbacks when only x and z can be measured, see [10].

Remark 6: The simpler controller $v_1 = -\zeta + \{\dddot{y}_d(t) + \kappa_2 \ddot{y}_d(t) + \kappa_1 \dot{y}_d(t)\}/\{2R_0(t)\}$ and the choice $\mu \equiv 0$ also make (8) UGAS to 0. This is seen by checking that the time derivative of the positive definite proper function

$$\begin{aligned} &V_o(e_1, e_2, \zeta) = A e_1^2 + e_2^2 + B e_1 e_2 + C(\zeta^2 + \zeta^4), \quad \text{where} \\ &A = \kappa_1 + \tfrac{B\kappa_2}{2}, \quad B = \min\left\{ \kappa_2, \sqrt{\kappa_1} \right\}, \quad \text{and} \\ &C = \max\left\{ \tfrac{1}{\kappa_2} + \tfrac{B}{4\kappa_1}, \tfrac{1}{4} + \tfrac{16\kappa_1 m_2}{\kappa_2} + 4Bm_2 \right\} \end{aligned}$$

along the solutions of $[\dot{e}_1 = e_2,\ \dot{e}_2 = -\kappa_1 e_1 - \kappa_2 e_2 + \zeta^2 + 2\zeta R_0,\ \dot{\zeta} = -\zeta]$ satisfies

$$\begin{aligned}
\dot{V}_o &= -B\kappa_1 e_1^2 + (B - 2\kappa_2)e_2^2 \\
&\quad +(2e_2 + Be_1)[\zeta^2 + 2\zeta R_0] - C(2\zeta^2 + 4\zeta^4) \\
&\leq -B\kappa_1 e_1^2 - \kappa_2 e_2^2 + \{\sqrt{\kappa_2}e_2\}\left\{\tfrac{2}{\sqrt{\kappa_2}}\left(\zeta^2 + 2\zeta R_0\right)\right\} \\
&\quad +B\{\sqrt{\kappa_1}e_1\}\left\{\tfrac{1}{\sqrt{\kappa_1}}(\zeta^2 + 2\zeta R_0)\right\} \\
&\quad -C(2\zeta^2 + 4\zeta^4) \quad (\text{since } B \leq \kappa_2) \\
&\leq -\tfrac{B\kappa_1}{2}e_1^2 - \tfrac{\kappa_2}{2}e_2^2 + \left[\tfrac{4}{\kappa_2} + \tfrac{B}{\kappa_1}\right](\zeta^4 + 4\zeta^2 R_0^2) \\
&\quad -C(2\zeta^2 + 4\zeta^4) \\
&\leq -\tfrac{B\kappa_1}{2}e_1^2 - \tfrac{\kappa_2}{2}e_2^2 - \tfrac{1}{2}\zeta^2,
\end{aligned}$$

where we used (6) and $pq \leq p^2/2 + q^2/2$ on the terms in braces. On the other hand, this simpler controller would not guarantee arbitrarily rapid local exponential convergence. The z^2 term in (1) gives rise to the constraint (5) on the feedback, which restricts the *global* convergence rate for e_1. Therefore, it would be useful for the control to, at least, produce arbitrarily rapid *local* convergence. For the proof that the feedback from Theorem 1 produces arbitrarily fast local exponential convergence, see [10].

IV. Proof of UGAS of (8) in Closed Loop with (14)

We prove that (8) with the feedback (14) has the Lyapunov function (15) if the a_is satisfy (13); see [10] for the rest of the proof of the theorem. Along the solutions of the *reduced* dynamics

$$\left\{\begin{aligned}
\dot{e}_1 &= e_2 \\
\dot{e}_2 &= -\kappa_1 e_1 - \tfrac{\kappa_1 m_1}{20}\sigma\left(\tfrac{20a_1}{\kappa_1 m_1}e_1\right) - \kappa_2 e_2 \\
&\quad -\tfrac{\kappa_1 m_1}{20}\sigma\left(\tfrac{20a_2}{\kappa_1 m_1}e_2\right),
\end{aligned}\right. \tag{16}$$

the function V_1 in (15) has time derivative $\dot{V}_1 \leq -\kappa_2 e_2^2$. By (I)-(II) from Remark 5 and simple calculations, the derivative of $T(e_1, e_2) = e_1 e_2$ along solutions of (16) yields

$$\begin{aligned}
\dot{T} &\leq e_2^2 - \kappa_1 e_1^2 + \left\{\tfrac{(\kappa_2 + a_2)|e_2|}{\sqrt{\kappa_1}}\right\}\left\{\sqrt{\kappa_1}|e_1|\right\} \\
&\leq \left(1 + \tfrac{(\kappa_2 + a_2)^2}{2\kappa_1}\right)e_2^2 - \tfrac{1}{2}\kappa_1 e_1^2,
\end{aligned} \tag{17}$$

by using the triangle inequality $pq \leq p^2/2 + q^2/2$ on the terms in braces. Thus, $\dot{V}_2 \leq -W_2(e_1, e_2)$ along the solutions of (16), where V_2 is from (15) and $W_2(e_1, e_2) = e_2^2 + \kappa_1 e_1^2/2$. Also, $V_2(e_1, e_2) \geq e_1 e_2 + K(e_2^2 + \kappa_1 e_1^2)/2 \geq K e_2^2/4 + K\kappa_1 e_1^2/4$ everywhere.

Using $\frac{\partial V_2}{\partial e_2}(e_1, e_2) = e_1 + Ke_2$, we get

$$\begin{aligned}
\dot{V}_2 &\leq -W_2(e_1, e_2) \\
&\quad +\tfrac{\partial V_2}{\partial e_2}(e_1, e_2)\left[\zeta^2 + 2\zeta R_\mu(e_1, e_2, t)\right] \\
&\leq -W_2(e_1, e_2) \\
&\quad +\sqrt{W_2(e_1, e_2)}\left\{\left[\tfrac{\sqrt{2}}{\sqrt{\kappa_1}} + K\right]\left[\zeta^2 + 2\overline{R}|\zeta|\right]\right\} \\
&\leq -\tfrac{1}{2}W_2(e_1, e_2) + \left[\tfrac{\sqrt{2}}{\sqrt{\kappa_1}} + K\right]^2(\zeta^4 + 4\overline{R}^2\zeta^2)
\end{aligned}$$

along the solutions of the full system (8), where we again used $pq \leq \frac{1}{2}p^2 + \frac{1}{2}q^2$ on the terms in braces. Recalling that $|\sigma'| \leq 1$ everywhere and (9) gives

$$\begin{aligned}
&\tfrac{1}{2\underline{R}}|\dot{\mu}| \leq \overline{L}(|e_1| + |e_2| + |\zeta| + \zeta^2), \quad \text{where} \\
&\overline{L} := \tfrac{1}{2\underline{R}}\{a_1 + a_2(1 + 2\overline{R} + \kappa_1 + \kappa_2 + a_1 + a_2)\}.
\end{aligned} \tag{18}$$

Hence, along the closed loop trajectories of (8), the time derivative for Q from (15) gives

$$\begin{aligned}
\dot{Q} &\leq -[\zeta^2 + \zeta^4 + \zeta^6] + \tfrac{1}{2\underline{R}a_3}(|\zeta| + |\zeta|^3)|\dot{\mu}| \\
&\leq -[\zeta^2 + \zeta^4 + \zeta^6] \\
&\quad +\tfrac{\overline{L}}{a_3}(|\zeta| + |\zeta|^3)(|e_1| + |e_2| + |\zeta| + \zeta^2) \\
&\leq -[\zeta^2 + \zeta^4 + \zeta^6] + \tfrac{\overline{L}}{a_3}(e_1^2 + e_2^2 + 2\zeta^2 + |\zeta|^3 \\
&\quad +\zeta^4 + |\zeta|^5 + \zeta^6) \\
&\leq -\left(1 - \tfrac{6\overline{L}}{a_3}\right)[\zeta^2 + \zeta^4 + \zeta^6] + \tfrac{\overline{L}}{a_3}(e_1^2 + e_2^2) \\
&\leq -\tfrac{1}{4}[\zeta^2 + \zeta^4] + \tfrac{1}{8\Gamma}\kappa_1 e_1^2 + \tfrac{1}{4\Gamma}e_2^2
\end{aligned} \tag{19}$$

by considering the possibilities $|\zeta| \geq 1$ and $|\zeta| < 1$, and then using $pq \leq \frac{1}{2}p^2 + \frac{1}{2}q^2$ and the fact that a_3 satisfies (13). Hence, our positive definite proper function V_3 in (15) gives $\dot{V}_3 \leq -\{W_2(e_1, e_2) + \zeta^2 + \zeta^4\}/4$ and therefore is a Lyapunov function for the system, which gives the UGAS assertion in the theorem.

V. Robustness Analysis

Next assume that the constant k in (1) is uncertain. This can be handled by replacing k with $k + \varepsilon m$ in (1), where k indicates an estimated or nominal value, ε is the uncertainty, and m is the electrode mass as before. We stipulate the admissible values of ε later. Our goal is to quantify the impact of ε on the tracking; see Remark 7 for the case where the parameter b is uncertain. To simplify arguments, we assume ε is constant, but analogous arguments apply for a general measurable essentially bounded uncertainty ε. With k replaced by $k + \varepsilon m$ in (1) and the same change of variables we used before, the feedback

$$\begin{aligned}
v_1 &= -\lambda^6\zeta(1 + \zeta^2) \\
&\quad +\tfrac{1}{2R_\mu(e_1, e_2, t)}\left\{\dddot{y}_d(t) + \kappa_2\ddot{y}_d(t) + \kappa_1\dot{y}_d(t)\right\}
\end{aligned} \tag{20}$$

with $\lambda > 0$ a constant we specify below (and with ζ, μ, R_μ, and y_d defined as before) gives the $Y = (e_1, e_2, \zeta)$ system

$$\left\{\begin{aligned}
\dot{e}_1 &= e_2 \\
\dot{e}_2 &= -\kappa_1 e_1 - \kappa_2 e_2 + \mu(e_1, e_2) + \zeta^2 \\
&\quad +2\zeta R_\mu(e_1, e_2, t) - \varepsilon(e_1 + y_d) \\
\dot{\zeta} &= -\lambda^6\zeta(1 + \zeta^2) - \tfrac{\dot{\mu}}{2R_\mu(e_1, e_2, t)}
\end{aligned}\right. \tag{21}$$

where the function μ will be chosen later to satisfy $|\mu(e_1, e_2)| \leq 0.5\kappa_1 m_1$ everywhere and we calculate $\dot{\mu}$ along the e-subdynamics of (21). We aim to show that μ can be selected so that the dynamics (21) is *input-to-state stable (ISS) with respect to* ε *with arbitrarily small linear overflows*. The relevant definitions are as follows.

We call (21) (with prescribed λ and μ) ISS with respect to ε provided that there are functions $\beta \in \mathcal{KL}$ and $\Delta \in \mathcal{K}_\infty$ so that all solutions $Y(t)$ of (21) for all initial values $Y(t_o)$ and all ε satisfy $|Y(t)| \leq \beta(|Y(t_o)|, t - t_o) + \Delta(|\varepsilon|)$ when $t \geq t_o \geq 0$.[1] When Δ has the form $\Delta(r) = \overline{\gamma} r$ for a constant $\overline{\gamma} > 0$, we call $\overline{\gamma}$ an *overflow rate*. The ISS inequality becomes the standard UGAS condition when ε is zero, but is far more general since its overshoot term $\Delta(|\varepsilon|)$ quantifies the impact of ε. Notice that ISS of (21) implies that $|e_1(t)| = |x(t) - y_d(t)| \to 0$ as $t \to +\infty$ with a small overshoot term when the uncertainty ε is suitably small.

We then say that (21) can be rendered ISS with respect to ε *with arbitrarily small linear overflows* provided that we can find a function $\beta \in \mathcal{KL}$ such that: For each choice of the constant $\overline{\gamma} > 0$, we can select our function μ and a constant $\lambda > 0$ (which, in general, both depend on $\overline{\gamma}$) such that all solutions $Y(t)$ of (21) for all choices of the initial state $Y(t_o)$ satisfy $|Y(t)| \leq \beta(|Y(t_o)|, t - t_o) + \overline{\gamma}|\varepsilon|$ whenever $t \geq t_o \geq 0$. This means that we can pick the controller to guarantee that the overflow rate $\overline{\gamma}$ is as small as desired.

To prove our ISS conditions, we use the Lyapunov function from Remark 6 except with $\zeta \equiv 0$, namely,

$$\begin{array}{l} \tilde{V}_o(e_1, e_2) = A e_1^2 + e_2^2 + B e_1 e_2, \ \text{ where} \\ A = \kappa_1 + \frac{B\kappa_2}{2} \ \text{ and } \ B = \min\left\{\kappa_2, \sqrt{\kappa_1}\right\}. \end{array} \tag{22}$$

Separately considering the possibilities $B = \kappa_2$ and $B = \sqrt{\kappa_1}$ leads easily to the global inequalities

$$\begin{array}{l} \omega_1(e_1^2 + e_2^2) \ \leq \ \tilde{V}_o(e_1, e_2) \ \leq \ \omega_2(e_1^2 + e_2^2), \ \text{ where} \\ \omega_1 = \frac{1}{2}\min\{\kappa_1, 1\} \ \text{and} \ \omega_2 = \max\{A, 1\} + \frac{B}{2}. \end{array} \tag{23}$$

To prescribe the allowable values of λ and ε, put

$$\begin{array}{l} \theta = \frac{c\omega_1}{20(4+B^2)}, \ \ c = \frac{\min\{B\kappa_1, \kappa_2\}}{B + 2\max\{A,1\}}, \\ M = \frac{1}{\theta}\max\left\{1, 4\overline{R}^2\right\}, \ \text{ and} \\ \tilde{\mathcal{L}} = \kappa_1 m_1 \left\{2(\kappa_1[m_1+1] + \kappa_2 + 2\overline{R}) + 3B\kappa_1 m_2 \right. \\ \qquad \left. + 2m_2 + 2 + B\right\}, \end{array} \tag{24}$$

where the m_is are from (3) and $\overline{R}$ is from (6). We assume that ε satisfies

$$|\varepsilon| \leq \min\left\{\frac{9B\kappa_1}{20(B+1)}, \frac{9\kappa_2}{20}, \frac{2\kappa_1 m_1}{5m_2}\right\} \tag{25}$$

but see Remark 7 for robustness results under less restrictive bounds on ε, and Section VI for an example where we compute our bounds explicitly. In [10], we prove:

Theorem 2: The choices $\sigma(s) = s/\sqrt{1+s^2}$ and

$$\mu(e_1, e_2) = -\frac{9}{20}\kappa_1 m_1 \sigma\left(\lambda \frac{\partial \tilde{V}_o}{\partial e_2}(e_1, e_2)\right) \tag{26}$$

with any constant $\lambda > 2 + \frac{9\tilde{\mathcal{L}}}{\underline{R}}(\frac{1}{\sqrt{c\omega_1}} + 1)(M+1)$ render (21) ISS with respect to uncertainties ε satisfying (25). In fact, by choosing μ as in (26) and λ appropriately, we can make (21) ISS with respect to ε with arbitrarily small linear overflows. Moreover, $V(e_1, e_2, \zeta) := \tilde{V}_o(e_1, e_2) + (M+1)(\zeta^4/4 + \zeta^2/2)$ is an ISS Lyapunov function for (21) when the uncertainty ε is constrained to satisfy (25).

Remark 7: The bound (25) implies arbitrarily small linear overflows in the ISS condition. If we only want to prove ISS of the dynamics (21) with respect to the uncertainty ε (with no restriction on the overflow rate for the ISS estimate), then we can use the less restrictive bound

$$|\varepsilon| \leq \min\left\{\frac{9B\kappa_1}{20(B+1)}, \frac{9\kappa_2}{20}\right\} \tag{27}$$

with the same μ from (26). For details, see [10].

Using similar reasoning, we can handle cases where the parameter b from (1) is uncertain. We model this case by replacing b with the uncertain value $b + \varepsilon m$ in (1), where ε represents the uncertainty and m is the movable electrode mass. Then we can show that the resulting closed loop dynamics with (26) satisfies the ISS condition with respect to additive uncertainties ε on $\kappa_2 = b/m$ satisfying

$$|\varepsilon| \leq \min\left\{\frac{\kappa_2}{5}, \frac{9\kappa_1}{20B}\right\}, \tag{28}$$

provided $\lambda > 0$ is a large enough constant; see [10] for the proof. Analogous results hold when the model has two independent (suitably small) parametric uncertainties, one on k and one on b.

VI. Simulations

To illustrate the efficacy of our approach, we simulated (1) with the feedback u from (7), μ given by (12), and v_1 from (14). We chose $a_1 = a_2 = 1$ and $a_3 = 100$. We used the parameters $m = 1$, $k = 2.5$, $\gamma = 1$, $b = 1$, $\alpha = 0.5$, $\beta = 0.001$, and $g_o = 1$, and the periodic C^3 reference trajectory

$$\begin{array}{rcl} y_d(t) & = & 0.01 + \varepsilon_1 \left[\mathcal{I}(500 + \min\{t, 50\})\right. \\ & & -\mathcal{I}(\min\{\max\{t, 450\}, 550\}) \\ & & \left. + \mathcal{I}(\max\{t, 950\} - 500)\right] \\ & & \quad \text{for } \ 0 \leq t \leq 1000, \\ y_d(t) & = & y_d(t - 1000) \ \text{ for } \ t \geq 1000, \end{array} \tag{29}$$

in which $\mathcal{I}(r) = \int_{450}^{r}(s - 450)^3(550 - s)^3 \mathrm{d}s$ and $\varepsilon_1 = .99/\mathcal{I}(550) = 1.386 \times 10^{-12}$. The function (29) is a smoothed standard square wave with offset 0.01 as shown in Figure 3. This mimics the periodic closing and opening of the relay. Conditions (3) are satisfied with $m_1 = 0.01$, $m_2 = 1$, $m_3 = 0.0216$, and $m_4 = 0.00074386$, which give $\underline{R} = 0.01249$ and $\overline{R} = \sqrt{5}$.

For the initial state $(x, \dot{x}, z)(0) = (0, 0, 10)$, we report our simulated error $e_1(t) = x(t) - y_d(t)$ in Figure 4. In Figures 5-6, we show the control u in its steady state and transient state. They illustrate how the tracking error rapidly converges to zero. The convergence also enjoys a desirable robustness to uncertainties in the parameters k and b. The bound in (27) is 0.45, which implies ISS convergence with respect to additive uncertainties ε on k, as long as $|\varepsilon|$ is kept below 18% of the value $k = 2.5$. Also, the bound from (28) is 0.2, which implies ISS with respect to uncertainties ε on b provided ε is below 20% of our nominal value $b = 1$.

[1] A function $\delta : [0, \infty) \to [0, \infty)$ is called *positive definite* provided that (A) $\delta(r) > 0$ for all $r > 0$ and (B) $\delta(0) = 0$. We write $\delta \in \mathcal{K}_\infty$ provided δ is positive definite, unbounded, and strictly increasing. We write $\beta \in \mathcal{KL}$ provided $\beta : [0, \infty) \times [0, \infty) \to [0, \infty)$ and (a) β is continuous, (b) for each $t \geq 0$, $\beta(\cdot, t) \in \mathcal{K}_\infty$, (c) for each $s \geq 0$, $\beta(s, \cdot)$ is nonincreasing, and (d) $\beta(s, t) \to 0$ as $t \to +\infty$ for each $s \geq 0$.

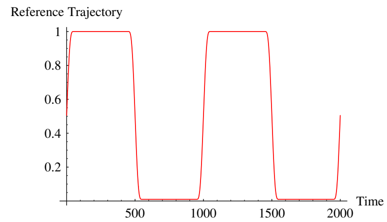

Fig. 3. Smoothed Square Wave $y_d(t)$ from (29)

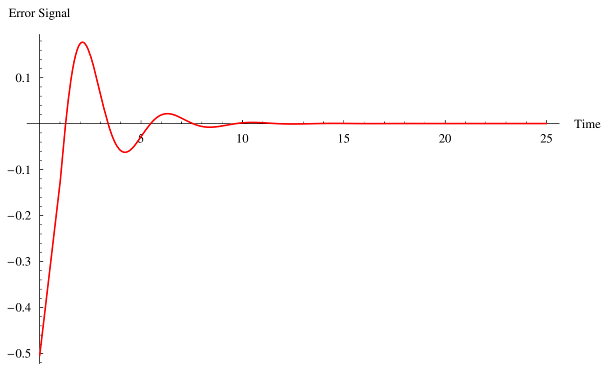

Fig. 4. Error $e_1(t) = x(t) - y_d(t)$

VII. Conclusions

We used Lyapunov function theory to design a family of nonlinear tracking feedback controllers for electromagnetic and electrostatic MEM relays. We established explicit conditions on the reference trajectory that guarantee that the trajectories can be tracked, and which are compatible with typical, alternating off-on relay operations. We then used ISS to quantify the robustness of our controllers to parametric uncertainty. The structure of the relay model precludes the construction of a tracking controller that gives global arbitrarily rapid exponential decay for the tracking error, but our proposed state feedback control has this property locally. Our numerical simulation illustrates the efficacy of our feedback control for a smoothed periodic square wave that mimics the periodic closing and opening of the relay.

References

[1] B. Borovic, C. Hong, A.Q. Liu, L. Xie, and F.L. Lewis, Control of a MEMS Optical Switch, in *Proc. Conf. Decision and Control*, Paradise Island, Bahamas, 2004, pp. 3039-3044.

[2] I.J. Busch-Vishniac, The Case for Magnetically Driven Microactuators, *Sensors and Actuators A*, no. 33, 1992, pp. 207-220.

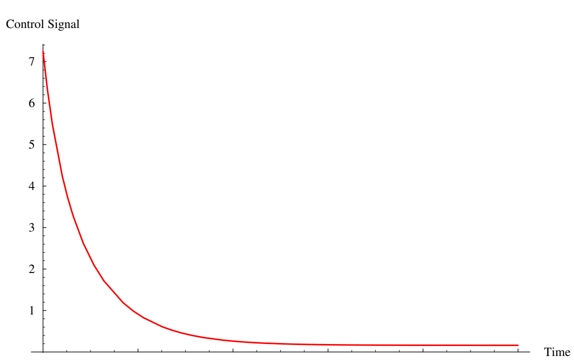

Fig. 5. Control Signal u in Transient State

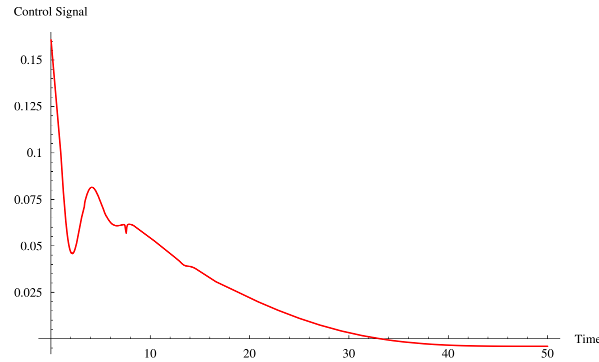

Fig. 6. Control Signal u Approaching Steady State

[3] H. Guckel, T. Earles, J. Klein, J.D. Zook, and T. Ohnstein, Electromagnetic Linear Actuators with Inductive Position Sensing, *Sensors and Actuators A*, no. 53, 1996, pp. 386-391.

[4] H. Hosaka, H. Kuwano, and K. Yanagisawa, Electromagnetic Microrelays: Concepts and Fundamental Characteristics, *Sensors and Actuators A*, no. 40, 1994, pp. 41-47.

[5] S.J. Jeong, *UV-LIGA Micro-Fabrication of Inertia Type Electrostatic Transducers and Their Application*, Ph.D. Dissertation, Louisiana State University, Baton Rouge, LA; 2005.

[6] H. Khalil, *Nonlinear Systems, Third Edition*, Prentice Hall, Englewood Cliffs, NJ; 2002.

[7] D.H.S. Maithripala, J.M. Berg, and W.P. Dayawansa, Capacitive Stabilization of an Electrostatic Actuator: An Output Feedback Viewpoint, in *Proc. American Control Conf.*, Denver, CO, 2003, pp. 4053-4058.

[8] D.H.S. Maithripala, J.M. Berg, and W.P. Dayawansa, Control of an Electrostatic Microelectromechanical System Using Static and Dynamic Output Feedback, *ASME J. Dynamic Systems, Measurement, and Control*, vol. 127, no. 3, 2005, pp. 443-450.

[9] D.H.S. Maithripala, B.D. Kawade, J.M. Berg, and W.P. Dayawansa, A General Modelling and Control Framework for Electrostatically Actuated Mechanical Systems, *Intl. J. Robust and Nonlinear Control*, vol. 15, 2005, pp. 839-857.

[10] M. Malisoff, F. Mazenc, and M. de Queiroz, Tracking and Robustness Analysis for Controlled Microelectromechanical Relays, *Intl. J. Robust and Nonlinear Control*, to appear. http://dx.doi.org/10.1002/rnc.1297

[11] B. McCarthy, G.G. Adams, N.E. McGruer, and D. Potter, A Dynamic Model, Including Contact Bounce, of an Electrostatically Actuated Microswitch, *J. Microelectromechanical Systems*, vol. 11, no. 3, 2002, pp. 276-283.

[12] R. Nadal-Guardia, A. Dehé, R. Aigner, and L.M. Castañer, Current Drive Methods to Extend the Range of Travel of Electrostatic Microactuators Beyond the Voltage Pull-In Point, *J. Microelectromechanical Systems*, vol. 11, no. 3, 2002, pp. 255-263.

[13] S.D. Senturia, *Microsystem Design*, Springer, New York; 2004.

[14] E.D. Sontag, Smooth Stabilization Implies Coprime Factorization, *IEEE Transactions on Automatic Control*, vol. 34, no. 4, 1989, pp. 435-443.

[15] E.D. Sontag, Input-to-State Stability: Basic Concepts and Results, in *Nonlinear and Optimal Control Theory*, P. Nistri and G. Stefani, eds., Springer Lecture Notes in Mathematics, Springer, Berlin, 2006, pp. 163-220.

[16] J.D. Williams, *Design and Fabrication of Electromagnetic Micro-Relays Using the UV-LIGA Technique*, Ph.D. Dissertation, Louisiana State University, Baton Rouge, LA; 2004.

[17] M. Younis, F. Gao, and M.S. de Queiroz, A Generalized Approach for the Control of MEM Relays, in *Proc. American Control Conf.*, New York, NY, July 2007, pp. 3180-3185.

[18] G. Zhu, J. Lévine, and L. Praly, Improving the Peformance of an Electrostatically Actuated MEMS by Nonlinear Control: Advances and Comparison, in *Proc. Conf. Decision and Control*, Seville, Spain, 2005, pp. 7534-7539.

[19] G. Zhu, J. Penet, and L. Saydy, Robust Control of an Electrostatically Actuated MEMS in the Presence of Parasitics and Parameter Uncertainties, in *Proc. American Control Conf.*, Minneapolis, MN, 2006, pp. 1233-1238.